OncoTargets and Therapy

Dovepress
open access to scientific and medical research

Open Access Full Text Article

ORIGINAL RESEARCH

GLUT-1 siRNA Enhances Radiosensitization Of Laryngeal Cancer Stem Cells Via Enhanced DNA Damage, Cell Cycle Redistribution, And Promotion Of Apoptosis In Vitro And In Vivo

Jiang-Tao Zhong[1]
Qi Yu[1]
Shui-Hong Zhou[1]
Er Yu[1]
Yang-Yang Bao[1]
Zhong-Jie Lu[2]
Jun Fan[3]

[1]Department of Otolaryngology, The First Affiliated Hospital, College of Medicine, Zhejiang University, Hangzhou, Zhejiang 310003, People's Republic of China; [2]Department of Radiotherapy, The First Affiliated Hospital, College of Medicine, Zhejiang University, Hangzhou, Zhejiang 310003, People's Republic of China; [3]State Key Laboratory for Diagnosis and Treatment of Infectious Diseases, the First Affiliated Hospital, College of Medicine, Zhejiang University, Hangzhou, Zhejiang 310003, People's Republic of China

Background: Radiotherapy does not show good efficacy against laryngeal cancer due to radioresistance. Cancer stem cells (CSCs) are considered among the causes of radioresistance. Inhibition of glucose transporter-1 (GLUT-1) using GLUT-1 small interfering RNA (siRNA) may enhance the radiosensitivity of laryngeal cancer cells, but the underlying cellular mechanisms remain unclear.

Methods: The $CD133^+$-Hep-2R cell line was established with repeated irradiation and magnetic-activated cell sorting. The effects of irradiation on $CD133^+$-Hep-2R cells were examined by CCK-8 assay, Transwell assay, quantitative real-time polymerase chain reaction (RT-PCR), and Western blotting. The effects of GLUT-1 siRNA on the radiosensitivity of $CD133^+$-Hep-2/2R cells were examined by RT-PCR, Western blotting, CCK-8 assay, colony formation assay, and Transwell assay in vitro and in a xenograft tumor model in nude mice. The cellular mechanism of enhanced radiosensitivity associated with GLUT-1 siRNA was investigated. The cell cycle and apoptosis rate were analyzed by flow cytometry, and the repair capability was examined by determining the levels of RAD51 and DNA-PKcs.

Results: $CD133^+$-Hep-2/2R cells showed stronger proliferation, lower apoptosis rate, lower percentage of G0/G1 phase cells, higher percentages of S and G2/M phase cells, and higher expression levels of GLUT-1 than Hep-2/2R cells. Transfection with GLUT-1 siRNA inhibited the proliferation and invasive capability of $CD133^+$-Hep-2R cells by inhibiting GLUT-1 expression, which also caused a redistribution of the cell cycle (higher proportion of cells in the G0/G1 phase and lower proportion in the S and G2/M phases), increased the apoptosis rate, and reduced DNA repair capability by suppressing RAD51 and DNA-PKcs expression.

Conclusion: The results of this study suggest that GLUT-1 siRNA can enhance the radiosensitivity of $CD133^+$-Hep-2R cells by inducing a redistribution of cell cycle phases, inhibiting DNA repair capability, and increasing apoptosis. Inhibition of GLUT-1 may have therapeutic potential for interventions to increase the radiosensitivity of laryngeal CSCs.

Keywords: glucose transporter-1, small interfering RNA, laryngeal cancer stem cells, radioresistance, DNA double-strand break

Correspondence: Shui-Hong Zhou
Department of Otolaryngology, The First Affiliated Hospital, College of Medicine, Zhejiang University, 310003, People's Republic of China
Tel +86-571-87236894
Fax +86-571-87236895
Email 1190051@zju.edu.cn

Introduction

Laryngeal cancer is one of the most common malignant tumors of the head and neck, and at diagnosis, about 60% of patients are already with stage III or IV disease and unfortunately, laryngeal cancer is one of a few oncologic diseases for which the 5-year survival rate has decreased over the past 40 years, from 66% to

submit your manuscript | www.dovepress.com
DovePress
http://doi.org/10.2147/OTT.S221423

63%, although the overall incidence is declining[1] This highlights the need for further research and innovation in this field. Radiotherapy shows poor efficacy against laryngeal cancer due to the radioresistance of these tumors. At present, there is no effective method to improve the radiosensitivity of laryngeal cancer in a clinical setting. Therefore, novel means of enhancing the radiosensitivity of laryngeal cancer are required to improve patient survival rate in clinical practice.

The therapeutic effects of radiotherapy are achieved by the induction of DNA double-strand breaks (DSBs), cellular apoptosis, and redistribution of the cell cycle.[2] DSBs are regarded as the most serious type of DNA damage induced by irradiation, as they cause cell death.[3,4] However, there are two major repair pathways for DSBs, homologous recombination (HR) and non-homologous end-joining (NHEJ), which may lead to radioresistance of tumor cells.[3] RAD51 is an important molecule in the HR pathway,[5] and DNA-dependent protein kinase, catalytic subunit (DNA-PKcs) plays a central role in the NHEJ pathway.[3] Agents targeting the DSB repair pathways that can enhance cellular apoptosis may improve the radiosensitivity of tumor cells.

Malignant tumor cells, including laryngeal cancer cells, mainly obtain energy via the glycolysis of glucose even under aerobic conditions. This aerobic glycolysis is termed the Warburg effect,[6,7] and is thought to be involved in the development of radioresistance in malignant tumors.[7–9] Glucose transporter-1 (GLUT-1), which is localized on the cell membrane and acts as a channel protein for the uptake of glucose in malignant tumor cells, has been shown to be a key regulator of the Warburg effect.[7,10] Previously, we reported that GLUT-1 is expressed at high levels in laryngeal cancer[11–13] and is involved in the development of radioresistance.[13–17] Inhibition of GLUT-1 using GLUT-1 antisense oligonucleotide (AS-ODN) and GLUT-1 small interfering RNA (siRNA) may enhance the radiosensitivity of laryngeal cancer cells.[13,15,17–19] However, the cellular mechanisms underlying the increased radiosensitivity of laryngeal cancer cells by GLUT-1 inhibitors remain unclear.

Cancer stem cells (CSCs) have high proliferative capacity and invasive ability, and are considered one of the causes of radioresistance in tumors.[20,21] CD133, a marker of CSCs,[22,23] is also found in laryngeal cancer cells and is associated with radioresistance.[24,25] In our previous study, we found that GLUT-1 is expressed at high levels in a Hep-2 laryngeal cancer cell line expressing high levels of CD133 ($CD133^+$-Hep-2),[26] and GLUT-1 siRNA improved the radiosensitivity of $CD133^+$-Hep-2 cells. There have been other studies on radioresistant Hep-2 (Hep-2R).[27,28] However, the correlation between high-level GLUT-1 expression and radioresistance in Hep-2R cells expressing high levels of CD133 ($CD133^+$-Hep-2R) has not been previously reported. In this study, we established the $CD133^+$-Hep-2R cell line, and used in vitro and in vivo models of laryngeal cancer to validate the radiosensitization effect of GLUT-1 siRNA on $CD133^+$-Hep-2R cells, investigating the cellular mechanisms underlying the enhancement of laryngeal cancer radiosensitivity by GLUT-1 siRNA.

Materials And Methods

Chemicals, Reagents, And Materials

Hep-2 cells were purchased from the Cell Research Institute of the Chinese Academy of Sciences (Shanghai, China). RPMI-1640 medium was obtained from Gibco-BRL (Gaithersburg, MD, USA). Fetal bovine serum was obtained from Hyclone (Logan, UT, USA). CD133 MicroBeads Kits were purchased from Miltenyi Biotec (Bergisch Gladbach, Germany). Anti-mouse CD133-PE antibody was purchased from Abcam (Cambridge, MA, USA). Cell Counting Kit-8 (CCK-8) kits were purchased from 7Sea Biotech (Shanghai, China). Annexin V kits were purchased from KeyGEN BioTECH (Jiangshu, China). TIANamp Genomic DNA Kits were purchased from Tiangen Biotech (Beijing, China). REeverAid™ first strand cDNA synthesis kits were purchased from Toyobo (Osaka, Japan). SYBR Green PCR kits were purchased from Thermo Scientific (Waltham, MA, USA). WesternBright™ ECL was purchased from Advansta (San Jose, CA, USA). Matrigel and Transwell chambers were purchased from Costar (Temecula, CA, USA). Anti-GLUT-1, anti-RAD5, anti-PKcs antibody was purchased from Abcam. GAPDH was purchased from Cell Signaling Technology (Beverly, MA, USA). Healthy male NOD/SCID nude mice (aged 4–6 weeks), weighing 18–20 g, were provided by Shanghai Sleek Laboratory Animal Co. Ltd. (Shanghai, China).

Cell Lines And Cell Culture

The human larynx squamous cell carcinoma Hep-2 cell line was cultured in RPMI-1640 supplemented with 10% heat-inactivated fetal bovine serum, 2 mM L-glutamine, 100 U/mL penicillin, and 100 μg/mL streptomycin at 37°C in a 5% CO_2 incubator. The cells were detached using 0.25%

trypsin plus 0.02% EDTA and harvested after reaching 80–90% confluence. The cell concentration was adjusted to 10^7 cells/mL. The radioresistant Hep-2R cell line was cultured using the same procedure as for the Hep-2 cell line.

Generation Of Hep-2R Cell Lines

Hep-2 cells in logarithmic growth phase were irradiated with X-rays (dose: 2 Gy; irradiation field size: 30 × 30 cm; source-skin distance: 80 cm; dose rate: 200 cGy/min) at room temperature, once daily, 5 days per week, for 3 weeks. Cells irradiated with a total dose of 30 Gy were collected and placed in an incubator.

Magnetic- And Fluorescence-Activated Cell Sorting Of $CD133^+$-Hep-2/2R Cells

Hep-2/2R cell suspensions incubated at 4°C for 30 min were labeled with anti-FcR receptor antibody and CD133-MicroBead kit sorting antibody (Miltenyi Biotec). After washing, labeled cells were loaded onto a column installed in a magnetic field. Trapped cells were collected as the $CD133_{high}$ fraction after the column was removed from the magnet. The collected cells were applied to a second column and the purification step was repeated. The flow-through fraction of the magnetic-activated cell sorting (MACS) column was used as the $CD133_{low}$ fraction. To assess the purity of the $CD133^+$-Hep-2/2R cells, anti-human CD133-PE was added to the cell suspension at concentrations suggested by the manufacturer and cells were incubated at 4°C in the dark for 10 min. After washing twice, paraformaldehyde (4%) was added to the mixture, which was fixed at 4°C for 20 min. The labeled cells were washed twice, suspended in phosphate-buffered saline (PBS), and analyzed by flow cytometry (Beckman, Fullerton, CA, USA).

GLUT-1 siRNA Transfection

GLUT-1 siRNA was purchased from GenePharma Co. Ltd. (Shanghai, China). The sequences were: sense, 5′-GGAAU UCAAUGCUGAUGAUTT-3′; antisense, 5′-AUCAUCAG CAUUGAAUUCCTT-3′. GLUT-1-siRNA transfection was performed when the cells reached 50% confluence in accordance with the manufacturer's protocol.

Irradiation

Cells were irradiated using a 6-MV linear accelerator (Clinac 23EX; Varian Inc., Palo Alto, CA) 24 h posttransfection. Irradiation treatment (source skin distance: 100 cm; radiation field: 35 × 35 cm; single X-ray dose: 6 MV; dose rate: 500 mU/min; and doses: 2, 4, 8, and 12 Gy) was performed in triplicate for each condition. Subsequently, the cells were cultured for 48 h.

Reverse Transcription Polymerase Chain Reaction (RT-PCR)

Aliquots of 1 μg of total RNA extracted from cells were used to synthesize first-strand cDNA using RevertAid first strand cDNA synthesis kits (Toyobo) according to the manufacturer's protocol. PCR amplification was carried out using 5 μL of cDNA as a template in a total reaction volume of 50 μL containing 16 μL deionized water, 25 μL SYBR Green Real-time PCR Master Mix, and 2 μL of each primer. The primers used were as listed for GLUT-1 (forward, 5′-GTCAACACGGCCTTCACTG-3′; reverse, 5′-GGTCATGAGTATGGCACAACC-3′), RAD51 (forward, 5′-AGGTGAAGGAAAGGCCATGTAC-3′; reverse, 5′-CATATGCTACATTATCCAGGACATCA-3′), PKcs (forward, 5′-CTAACTCGCCAGTTTATCAATC-3′; reverse, 5′-TTTTTCCAATCAAAGGAGGG-3′) and GAPDH (forward, 5′-GAGCCCGCAGCCTCCCGCTT-3′; reverse, 5′-CCCGCGGCCATCACGCCACAG-3′). Following a 10-min denaturation step at 95°C, the reactions were performed for 40 cycles of denaturation for 10 s at 95°C, annealing at 60°C for 20 s, and extension at 72°C for 30 s, followed by a final extension at 72°C for 10 min.

Western Blotting

The proteins were extracted with RIPA lysis buffer containing several protease and phosphatase inhibitors. The proteins were separated using SDS-polyacrylamide gel electrophoresis and transferred onto polyvinylidene difluoride (PVDF) membranes (item no: IPVH00010; Millipore Co., Boston, MA, USA). Immunoblotting was carried out using monoclonal antibodies: anti-GLUT-1 (cat no. ab40084, 1:200; Abcam), anti-RAD51 (cat no. Ab88572, 1:200; Abcam), anti-PKcs (cat no. Ab70250, 1:200; Abcam), and anti-GAPDH (cat. no. AP0063, 1:4000; Bioworld, Dublin, OH, USA). The membranes were then incubated with secondary antibody, detected using an ECL chemiluminescence assay kit (Beyotime Biological Technology Co. Ltd., Shanghai, China), and visualized by X-ray film exposure. Protein expression was analyzed semiquantitatively using the ChemiDoc XRS+ System (Bio-Rad, Hercules, CA, USA).

Cell Proliferation Assay

For the Cell Counting Kit-8 assay (CCK-8), cells were seeded at a density of 3000–3500 cells/well in 96-well plates and cultured for 48 h. Subsequently, cells were incubated in the dark for 1 h after adding cell counting solution (10 μL). The absorption of each well was measured at 450 nm using a Spectra Plus microplate reader (Molecular Devices Co., Sunnyvale, CA, USA). For cell growth assays, cells were seeded at a density of 1×10^5 cells/well in 25-cm^2 culture flasks. The number of viable cells was determined at different time points. For colony formation assays, cells were seeded in 6-well plates at a density of 800–1000 cells/well and cultured for 12 h, followed by irradiation with X-rays (0, 2, 4, 6, 8, or 12 Gy). After incubation for a further 10 days, colonies were stained with 0.5% crystal violet for 20 min and counted.

Detection Of Apoptosis

For the in vitro study, $CD133^+$-Hep-2/2R cells were cultured for 48 h in a humidified atmosphere containing 5% CO_2 and digested with trypsin. For the in vivo study, the tumor tissue was washed and cut into small pieces. The separated cells were collected after milling with a syringe plunger, filtered using a 400-mesh sieve, and digested using trypsin without EDTA. Apoptosis was assessed by flow cytometry. Populations of apoptotic cells were determined by staining cells with annexin V-fluorescein isothiocyanate (FITC) and propidium iodide (PI; Sigma, St. Louis, MO, USA) according to the manufacturer's protocol (annexin V kit; KeyGEN BioTECH). Briefly, the cells were resuspended in binding buffer and stained with annexin V-FITC and PI for 10 min in the dark at room temperature. The cell suspension was immediately analyzed by flow cytometry. The data were analyzed using ModFit LT software (Becton Dickinson, Mountain View, CA, USA). Each experiment was performed in triplicate.

Transwell Assays

The migratory potential of cells was measured using Transwell assays. Briefly, Matrigel (Costar) was melted, diluted with serum-free medium, and added to the center of a Transwell chamber (Costar), followed by incubation at 37°C for 4–5 h to allow gelatinization. Cells (5×10^4) were seeded onto the upper chamber of the Transwell chamber in serum-free medium and incubated for 24 h for invasion. The cells were fixed in methanol at room temperature for 20 min and stained with 2% crystal violet at room temperature for 30 min. The filters were washed with PBS and the upper cells were removed with cotton-tipped swabs. The cells on the underside of the filters were counted and photographed using an inverted microscope. Each experiment was repeated at least three times.

Tumor Xenograft Model

Male NOD/SCID nude mice (aged 4–6 weeks) provided by the Shanghai Sleek Laboratory Animal Co. Ltd. (Shanghai, China) were housed under specific pathogen-free conditions according to the institutional guidelines for animal care. All animal experiments were approved by the institutional review board of the First Affiliated Hospital, College of Medicine, Zhejiang University (Hangzhou, Zhejiang, China). To establish a laryngeal cancer mouse model, 4×10^6 cells (Hep-2/2R and $CD133^+$-Hep-2/2R cells) in 200 μL of PBS were injected subcutaneously into the flanks of nude mice. RPMI-1640, siRNA-NC, or GLUT-1 siRNA was injected peritumorally into the nude mice at a dose of 4 mL/kg per mouse on days 10, 13, 17, 20, and 24 after inoculation. After intraperitoneal injection of 4% chloral hydrate at a dose of 7 mL/kg, the tumors were subsequently exposed to local irradiation at a dose of 1 Gy on the corresponding days. The cumulative local radiation dose was 5 Gy per mouse. The mice were divided into one group for Hep-2/2R cells (treatment with RPMI-1640) and five groups for $CD133^+$-Hep-2/2R cells (treatment with RPMI-1640, RPMI-1640+X-ray, siRNA-NC, GLUT-1-siRNA and GLUT-1-siRNA+X-ray), consisting of three mice per group. Tumor sizes were measured every 4 days using an electronic digital caliper, and tumor volume was calculated using the formula: $V = 1/2\times(\text{largest diameter})\times(\text{smallest diameter})^2$. The nude mice were sacrificed on day 26 and the tumors were dissected, weighed, and snap-frozen for protein expression analysis.

Analysis Of Cell Cycle Distribution By Flow Cytometry

The separated cells of the tumor tissue were collected as described above. The cells were fixed in precooled 70% alcohol (2 mL) overnight at −20°C, washed twice with ice-cold PBS, resuspended in PBS (500 μL) with RNase A (10 μL, 50 μg/mL) at 37°C for 30 min, stained with PI (50 μg/mL) at room temperature for 30 min in the dark, and analyzed by flow cytometry. Each experiment was performed at least twice.

Statistical Analysis

Results shown are representative of at least three separate experiments. Comparisons between groups were performed using Student's *t*-test and one-way or two-way analysis of variance (ANOVA) using SPSS software (ver. 19.0 for Windows; SPSS Inc., Chicago, IL, USA). All statistical data are presented as the mean ± SD. In all analyses, $P < 0.05$ was taken to indicate statistical significance.

Results

CD133$^+$-Hep-2R Cell Line Was Successfully Established

To obtain the Hep-2R cell line, Hep-2 cells were irradiated repeatedly. Analysis of cell growth was used to assess the proliferative capacity of Hep-2R cells. As shown in Figure 1A, Hep-2R cells showed weaker proliferative capacity than Hep-2 cells. To validate that Hep-2R was more irradiation resistant than Hep-2, Hep-2R and Hep-2 were irradiated with different doses of X-ray (0, 2, 4, 6, 8, 10 Gy) and the number of survived cells was measured according to the method mentioned in "Irradiation" and "Cell proliferation assay" parts of the "Material and Methods" section. The results were shown in Figure 1B: under different doses of irradiation, Hep-2R demonstrated more survived cells than Hep-2. Furthermore, the IC50 was calculated based on the data presented in Figure 1B: for Hep-2, IC50=3.392 Gy; for Hep-2R, IC50=8.049 Gy. So the above results demonstrated that Hep-2R was more irradiation resistant than Hep-2.

In the next, to obtain the CD133$^+$-Hep-2R cell line, Hep-2R cells expressing CD133 were sorted by MACS. Flow cytometry was performed to assess the proportion of CD133$^+$-Hep-2R cells. As shown in Figure 1C, the proportion of CD133$^+$-Hep-2R cells increased significantly after MACS ($P < 0.01$).

Differences In Tumor Characteristics Between CD133$^+$-Hep-2/2R Cells And Hep-2/2R Cells

To evaluate the differences in tumor characteristics between CD133$^+$-Hep-2/2R cells and Hep-2/2R cells, we established Hep-2/2R and CD133$^+$-Hep-2/2R xenograft models in nude mice. The xenograft tumor volumes were calculated to assess proliferation. As shown in Figure 2A, the volume of the CD133$^+$-Hep-2/2R xenograft tumors was significantly greater than that of Hep-2/2R xenograft tumors ($P < 0.01$). Flow cytometry was performed to evaluate the apoptosis rate and changes in the cell cycle distribution of CD133$^+$-Hep-2/2R cells. As shown in Figure 2B, the apoptosis rate was significantly reduced in CD133$^+$-Hep-2/2R cells compared to that in Hep-2/2R cells ($P < 0.01$). As shown in Figure 2C, cell cycle analysis indicated that the proportion of CD133$^+$-Hep-2R cells at G0/G1 phase was significantly decreased ($P < 0.01$), which was accompanied by significantly increased proportions of cells in S ($P < 0.01$) and G2/M ($P < 0.05$) phases, compared to Hep-2R cells. For CD133$^+$-Hep-2 cells, the proportion of cells at S phase was significantly increased compared to that in Hep-2 cells ($P < 0.05$), but there were no significant differences in the proportions of cells at G0/G1 and G2/M phases between the two cell lines. We further assessed the expression levels of GLUT-1 by RT-PCR and Western blotting. As shown in Figure 2D and E, the levels of GLUT-1 mRNA and protein expression were significantly greater in CD133$^+$-Hep-2/2R cells than in Hep-2/2R cells ($P < 0.01$). The above results indicate that CD133$^+$-Hep-2/2R cells had stronger proliferative activity, lower apoptosis rate, lower percentage of G0/G1-phase cells, higher percentage of S and G2/M-phase cells, and higher levels of GLUT-1 expression than Hep-2/2R cells.

Effects Of Irradiation On CD133$^+$-Hep-2R Cells

To evaluate the effects of irradiation on CD133$^+$-Hep-2R cells, the cells were exposed to different doses of irradiation. CCK-8 assays and clonogenic survival assays were performed to assess the proliferative capacity of CD133$^+$-Hep-2R cells. As shown in Figure 3A and B, in response to increasing irradiation doses, the cell viability and cell proliferation rate of CD133$^+$-Hep-2R cells increased at 2 and 4 Gy, but decreased at 8 and 12 Gy. The invasive capability of CD133$^+$-Hep-2R cells was assessed by Transwell assays. As shown in Figure 3C, the number of migrated cells did not decrease significantly at lower irradiation doses, whereas it increased at 8 Gy. These results suggest that CD133$^+$-Hep-2R cells showed radioresistance.

RT-PCR and Western blotting were performed to evaluate the effects of irradiation on GLUT-1 expression in CD133$^+$-Hep-2R cells. As shown in Figure 3D and E, following irradiation, GLUT-1 mRNA and protein expression were significantly increased at 2 and 4 Gy ($P < 0.01$),

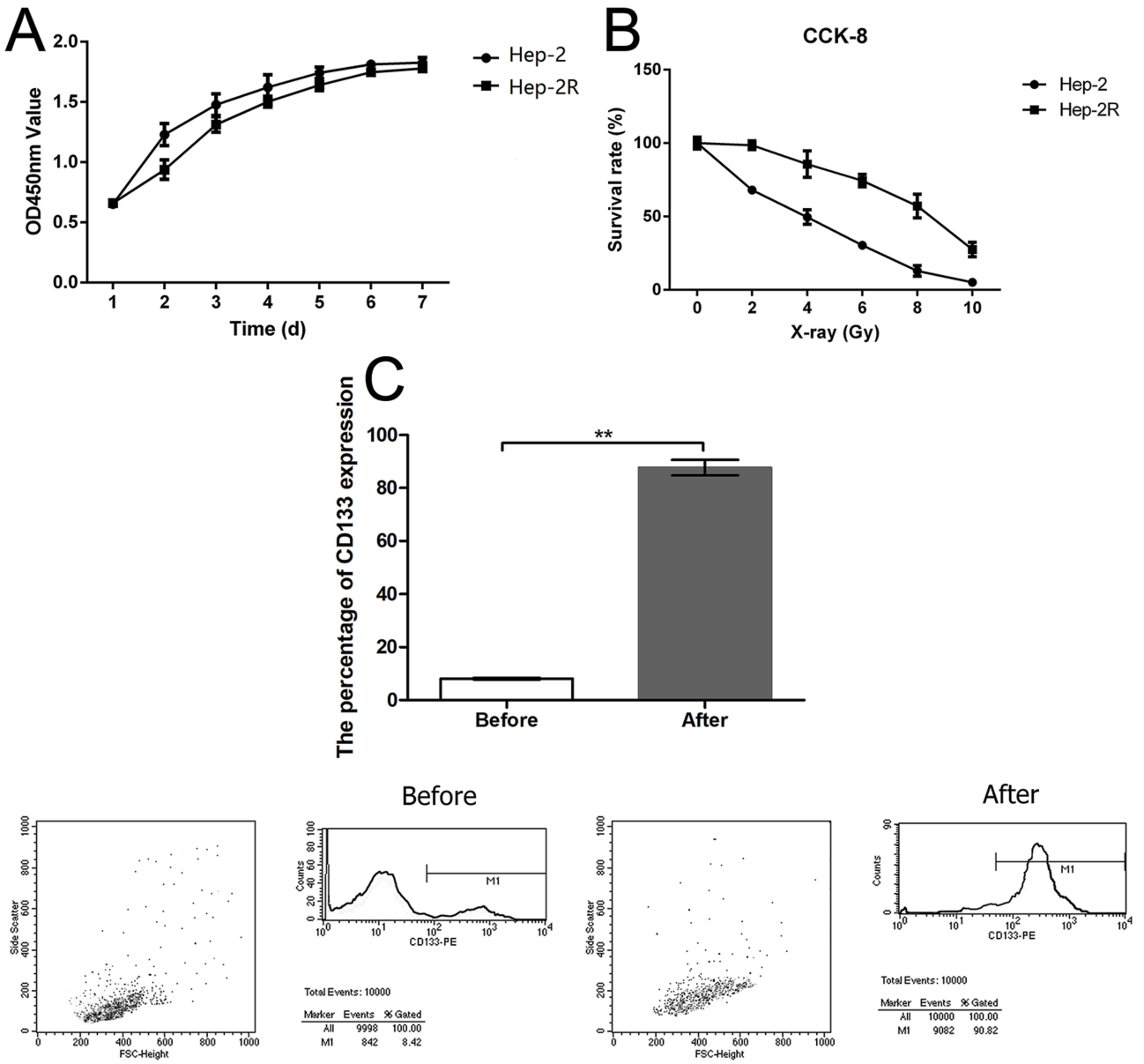

Figure 1 Establishment of Hep-2R and CD133$^+$-Hep-2R cell lines. (**A**) Optical density at 450 nm (OD_{450}) of Hep-2 and Hep-2R cells as a measure of the doubling time (Hep-2, 40.7 h; Hep-2R, 48.4 h). (**B**) The comparison of irradiation resistance between of Hep-2R and Hep-2 cell lines. (**C**) Establishment of CD133$^+$-Hep-2R cell line through magnetic-activated cell sorting (MACS) and flow cytometry. **: p<0.01.

and significantly decreased at 8 Gy ($P < 0.01$), suggesting that the radioresistance of CD133$^+$-Hep-2R cells may be mediated by increased GLUT-1 expression.

GLUT-1 siRNA Enhances The Radiosensitivity Of CD133$^+$-Hep-2/2R Cells

To determine whether GLUT-1 is a key factor in the radioresistance of CD133$^+$-Hep-2R cells, we inhibited GLUT-1 expression using GLUT-1 siRNA. As shown in Figure 3D and E, RT-PCR and Western blotting analyses indicated that GLUT-1 mRNA and protein expression were significantly decreased by irradiation, with the most pronounced decrease at 12 Gy ($P < 0.01$). To further determine the effects of GLUT-1 siRNA on radiosensitivity, CD133$^+$-Hep-2R cells were pretreated with GLUT-1 siRNA and exposed to different doses of irradiation followed by CCK-8 assay and clonogenic survival assay to assess their proliferative capacity. As shown in Figure 3A and B, the cell viability and cell proliferation rate of CD133$^+$-Hep-2R cells transfected with GLUT-1 siRNA were lower than

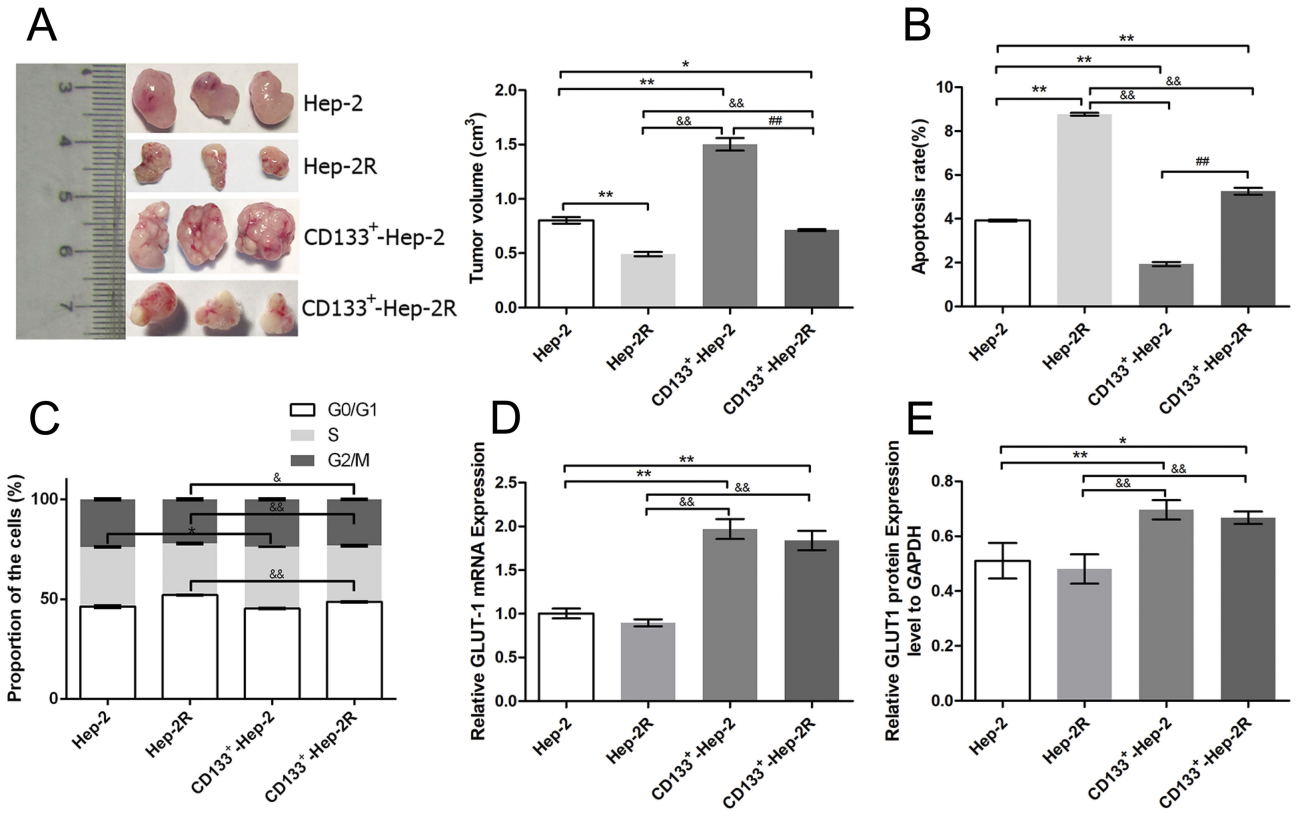

Figure 2 Differences in tumor characteristics between CD133$^+$-Hep-2/2R cells and Hep-2/2R cells. (**A**) Volumes of xenograft tumors. (**B**) Rates of apoptosis. (**C**) Proportions of cells in different phases. (**D**) GLUT-1 mRNA expression levels. (**E**) GLUT-1 protein expression levels vs those in Hep-2 cells. **, &&, ##: p<0.01; *, &: p<0.05.

those in the negative control group ($P < 0.01$). Transwell assays were performed to assess the invasive capacity of CD133$^+$-Hep-2R cells. As shown in Figure 3C, the number of migrated cells was significantly lower in the cells transfected with GLUT-1 siRNA than in the negative control group ($P < 0.01$). These results suggest that transfection with GLUT-1 siRNA may inhibit the proliferative and invasive capabilities of CD133$^+$-Hep-2R cells via inhibition of GLUT-1 expression, which may enhance the radiosensitivity of CD133$^+$-Hep-2R cells.

In addition to the in vitro experiments, we also conducted in vivo experiments. We established a CD133$^+$-Hep-2/2R xenograft model in nude mice, and divided them into five treatment groups: blank, X-ray, siRNA-NC, GLUT-1-siRNA, and GLUT-1-siRNA+X-ray. As shown in Figure 4A and B, the levels of GLUT-1 mRNA and protein expression were significantly decreased after irradiation ($P < 0.05$) or treatment with GLUT-1 siRNA ($P < 0.05$) alone, and the decreases were most pronounced after treatment with a combination of irradiation and GLUT-1 siRNA ($P < 0.05$). The xenograft tumor volumes were calculated to assess proliferation. As shown in Figure 4C, the volumes of the xenograft tumors were significantly reduced in the X-ray ($P < 0.01$) and GLUT-1-siRNA ($P<0.05$) groups compared with blank and siRNA-NC groups, respectively, with the most pronounced decrease seen in the GLUT-1-siRNA+X-ray group ($P < 0.05$). Taken together, these findings suggest that transfection with GLUT-1 siRNA increased the radiosensitivity of CD133$^+$-Hep-2/2R cells.

GLUT-1 siRNA Regulates The Cell Cycle In CD133$^+$-Hep-2/2R Cells

To verify whether GLUT-1 siRNA increases radiosensitivity by redistributing the cell cycle, the cell cycles of CD133$^+$-Hep-2/2R cells in xenograft tumors were analyzed using flow cytometry. As shown in Figure 5A, after irradiation or GLUT-1 siRNA treatment alone, the proportion of cells in xenograft tumors in the G0/G1 phase increased, whereas the proportions of cells in the S and G2/M phases decreased significantly in comparison to the controls ($P < 0.05$). We further treated the xenograft tumors with irradiation and GLUT-1 siRNA together, and the proportion of cells in the G0/G1 phase was higher and those in the S and G2/M phases were lower than in the single-treatment X-ray and GLUT-1-siRNA groups

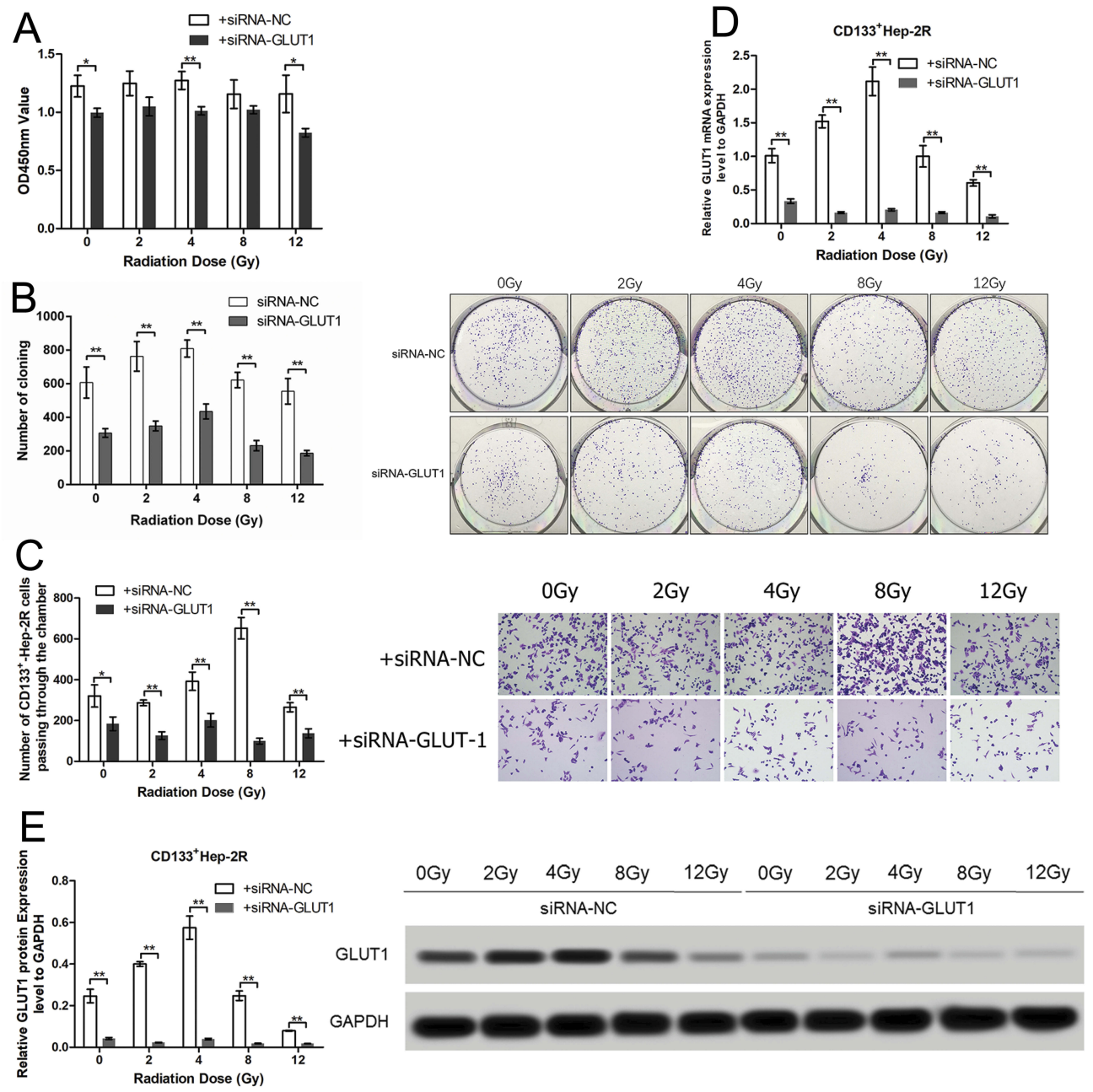

Figure 3 Effects of irradiation and GLUT-1 siRNA on CD133$^+$-Hep-2R cells. (**A**) Optical density at 450 nm (OD_{450}) of CD133$^+$-Hep-2R cells in CCK-8 assays. (**B**) Colony forming images and numbers of clones in clonogenic survival assays. (**C**) Number of CD133$^+$-Hep-2R cells passing through the chamber in Transwell assays. (**D**) GLUT-1 mRNA expression levels. (**E**) GLUT-1 protein expression levels. **: p<0.01, *: p<0.05.

($P < 0.05$). These results suggest that GLUT-1 siRNA redistributed the cell cycle, enhancing the effects of irradiation.

Irradiation Combined With GLUT-1 siRNA Promotes Apoptosis

To further investigate whether GLUT-1 siRNA enhances the radiosensitivity of CD133$^+$-Hep-2/2R cells by increasing apoptosis induced by irradiation, the apoptosis rate was analyzed by flow cytometry. As shown in Figure 5B and C, in the in vitro experiments, the apoptosis rate of CD133$^+$-Hep-2R cells transfected with GLUT-1 siRNA was significantly higher than that of the control group ($P < 0.01$). In the in vivo experiments, the apoptosis rate of CD133$^+$-Hep-2/2R cells in xenograft tumors was significantly increased after treatment with irradiation ($P < 0.01$) or GLUT-1 siRNA ($P < 0.01$), and further increased by combined treatment with irradiation and GLUT-1 siRNA ($P < 0.01$). These findings suggest that

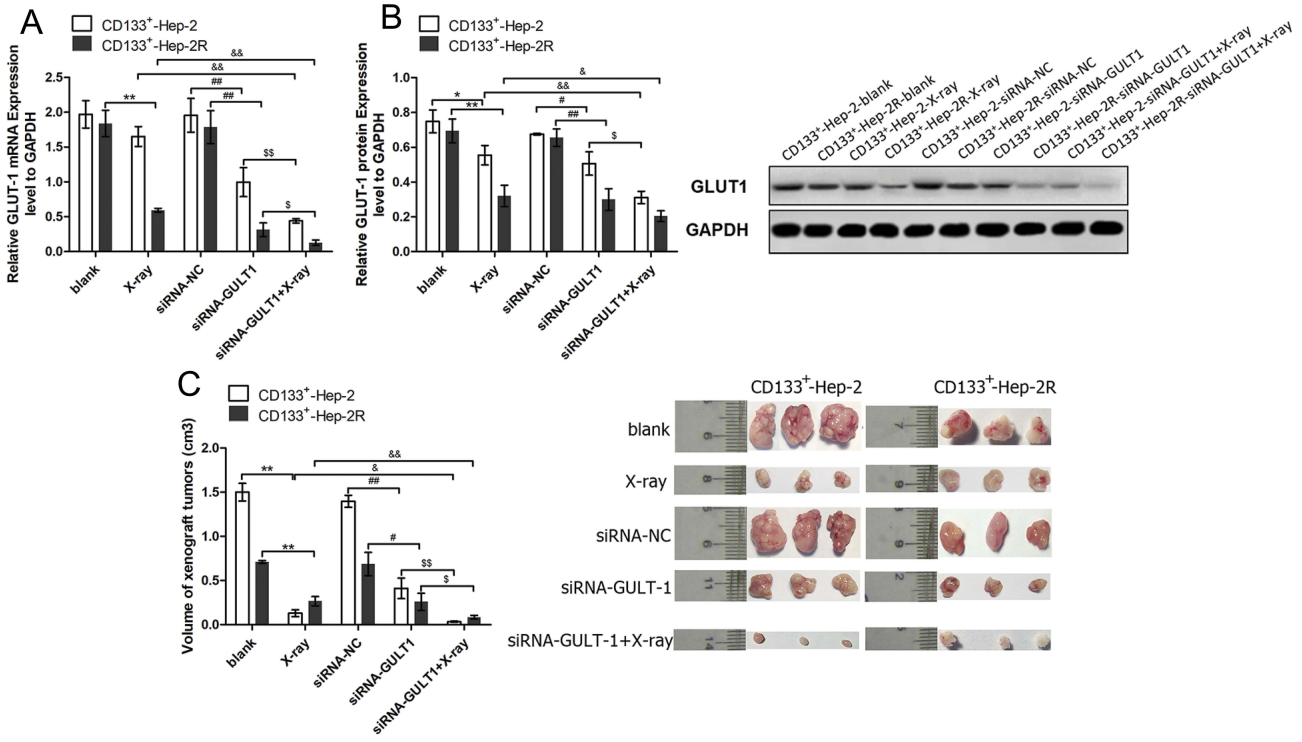

Figure 4 GLUT-1 siRNA enhances the radiosensitivity of CD133$^+$-Hep-2/2R cells. (**A**) GLUT-1 mRNA expression levels. (**B**) GLUT-1 protein expression levels. (**C**) Volumes of xenograft tumors. **, &&, ##, $$: p<0.01; *, &, #, $: p<0.05.

apoptosis caused by irradiation was enhanced by transfection with GLUT-1 siRNA.

GLUT-1 siRNA Reduced DNA Repair Capability In CD133$^+$-Hep-2/2R Cells

DSBs are a lethal form of DNA damage, and are primarily responsible for cell death during radiotherapy[3] The radiosensitivity of CD133$^+$-Hep-2/2R cells may be enhanced by the combination of irradiation with a specific agent targeting DSB repair. As RAD51 and DNA-PKcs play important roles in major repair pathways for DSBs, the repair capability was examined by determining the levels of RAD51 and DNA-PKcs in CD133$^+$-Hep-2/2R cells. As shown in Figure 5D and F in the in vitro experiments, RAD51 and DNA-PKcs levels in CD133$^+$-Hep-2R cells transfected with GLUT-1 siRNA were significantly reduced by irradiation compared to levels in the control group ($P < 0.01$). As shown in Figure 5E and G, in the in vivo experiments, the mRNA and protein levels of RAD51 and DNA-PKcs in CD133$^+$-Hep-2 cells were significantly reduced after treatment with irradiation ($P < 0.01$) or GLUT-1 siRNA ($P < 0.01$), and a greater reduction was observed in cells treated with a combination of irradiation plus GLUT-1 siRNA ($P < 0.01$). These findings suggest that treatment with GLUT-1 siRNA impaired the ability to repair DNA damage induced by irradiation.

Discussion

Radiotherapy plays an important role in the treatment of laryngeal cancer. However, the development of radioresistance leads to disease recurrence and poor prognosis. The mechanisms underlying radioresistance in laryngeal cancer remain unclear. Current hypotheses to explain radioresistance include laryngeal CSCs, irradiation damage repair capability, differences in the cell cycle, hypoxia, signaling pathways, and clinically relevant factors. CD133 expression was reported in intrahepatic cholangiocarcinoma, liver cancer, glioma, and renal cancer[22] CD133 was also shown to be highly expressed in CSCs in head and neck malignant tumors, and to play a role in the development of radioresistance.[29–33] The laryngeal squamous cell carcinoma cell lines Hep-2 and TU-177 expressing CD133 showed stronger tumorigenic characteristics, including greater cell viability, invasiveness, colony forming capability, and resistance to radiation[25] In the present study, we sorted laryngeal CSCs expressing CD133 by flow cytometry and found that CD133$^+$-Hep-2/2R cells showed stronger proliferative capability, a lower rate of apoptosis,

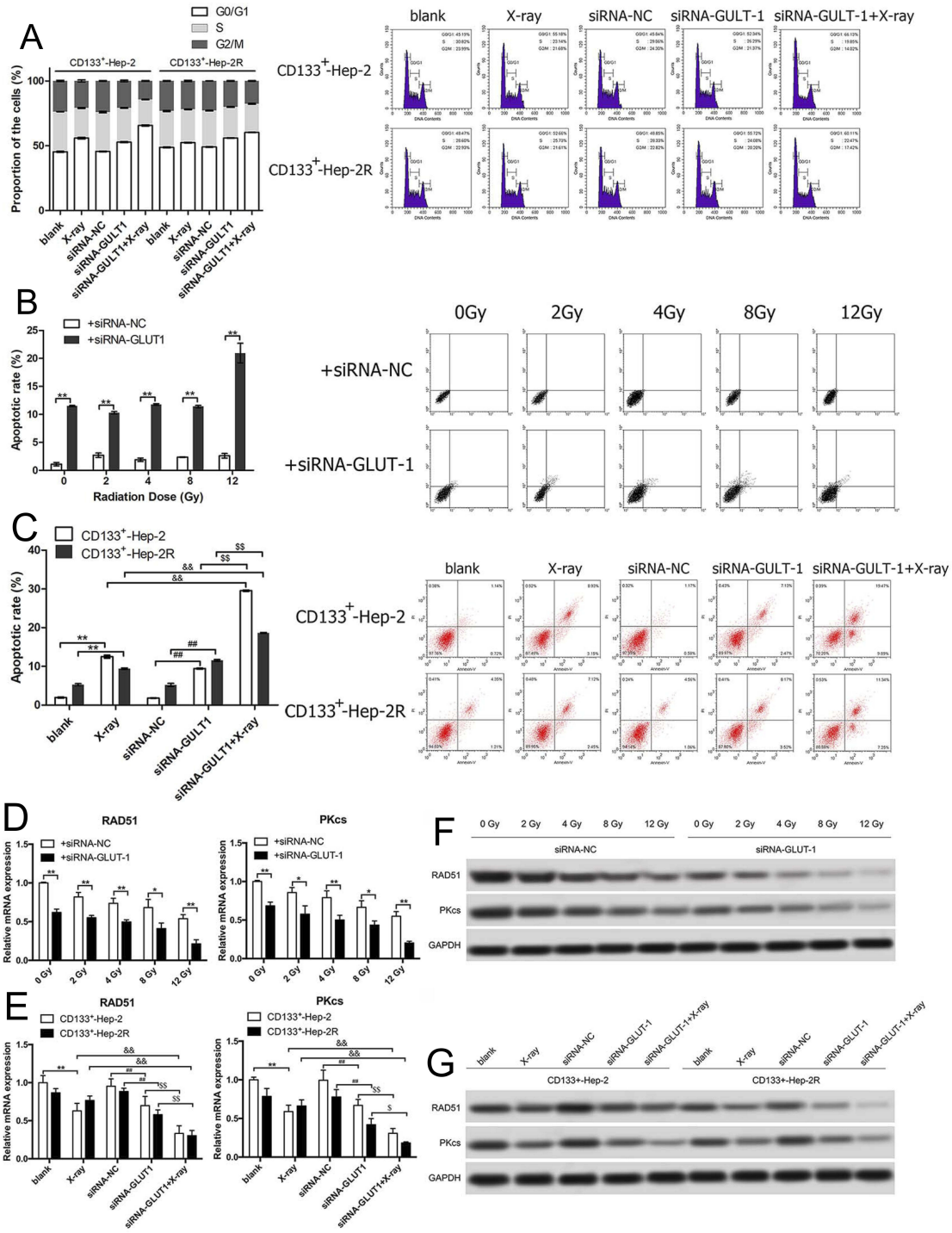

Figure 5 GLUT-1 siRNA regulates the cell cycle, promotes apoptosis, and reduces DNA repair capability in CD133$^+$-Hep-2/2R cells. (**A**) Proportions of cells in different phases of the cell cycle. (**B**) Rate of apoptosis of CD133$^+$-Hep-2R cells. (**C**) Rate of apoptosis of xenograft tumors. (**D**) RAD51 and PKcs mRNA levels in CD133$^+$-Hep-2R cells. (**E**) RAD51 and PKcs mRNA levels in xenograft tumors. (**F**) RAD51 and PKcs protein levels in CD133$^+$-Hep-2R cells. (**G**) RAD51 and PKcs protein levels in xenograft tumors. **, &&, ##, $$: p<0.01; *, #, $: p<0.05.

lower percentage of G0/G1-phase cells, higher percentages of S and G2/M-phase cells, and higher expression levels of GLUT-1 than Hep-2/2R cells.

To determine the radioresistance of CD133$^+$-Hep-2R cells, the cells were exposed to different doses of irradiation and their proliferative capacity was assessed by CCK-8

assays and clonogenic survival assays. The results showed that low-dose irradiation increased the proliferation of CD133$^+$Hep-2R cells, and there was no decrease in their survival or invasive capability. High-dose irradiation reduced cell proliferation, clonogenic survival rate, and invasion. The results indicated that CD133$^+$-Hep-2R cells obtain radioresistance on exposure to low-dose irradiation. Cells show transient responses after irradiation, including aging, apoptosis, necrosis, and autophagy.[34] In low-dose irradiation, cells exhibit autophagy, DNA repair, and cell cycle arrest. Consequently, the proliferation of cells is slowed, and radioresistance develops in these cells. Tumor cells reproliferate after DNA repair, which is one of the mechanisms through which tumors develop radioresistance. It has been reported that low-dose (0.1–2 Gy) irradiation increases proliferation and invasion and inhibits apoptosis in mesenchymal stem cells.[35] Similar observations were also reported in CSCs.[35] The effectiveness of irradiation depends on the balance between DNA damage and DNA repair.[36] When DNA damage is greater than DNA repair, radiotherapy is effective and the cells undergo apoptosis and death. In high-dose irradiation, the degree of DNA damage in the cell exceeds its DNA repair capability, leading to senescence, apoptosis, and necrosis[34] These results were corroborated by the findings of the present study.

As GLUT-1 is involved in the development of radioresistance, we further evaluated GLUT-1 expression in CD133$^+$Hep-2R cells by RT-PCR and Western blotting. GLUT-1 expression was shown to increase with low-dose irradiation, but to decrease with high-dose irradiation, indicating the same trend as observed for cell proliferation and invasion. Therefore, we hypothesized that CD133$^+$Hep-2R cells show resistance to the damage caused by low-dose irradiation through increased expression of GLUT-1, leading to the development of radioresistance. To validate this hypothesis, we inhibited GLUT-1 expression by transfecting CD133$^+$Hep-2R cells with GLUT-1 siRNA. The in vitro experiments showed that even after low-dose irradiation, the proliferation, colony forming efficiency, and invasive capability of cells were inhibited in an irradiation dose-dependent manner. Furthermore, the in vivo experiments showed that the volumes of xenograft tumors treated with combined irradiation and transfection with GLUT-1 siRNA were significantly reduced. These results suggested that GLUT-1 siRNA may increase the radiosensitivity of radioresistant laryngeal CSCs. Consistent with the results presented here, earlier studies also showed that GLUT-1 AS-ODN and GLUT-1 siRNA enhanced the radiosensitivity of laryngeal cancer cells,[13,15,17–19] but the cellular mechanisms underlying these effects remain unclear.

We first performed cell cycle analysis using flow cytometry to determine whether GLUT-1 siRNA enhances the radiosensitivity of CD133$^+$Hep-2R cells through redistribution of the phases of the cell cycle. Both irradiation and GLUT-1 siRNA significantly affected the cell cycle in CD133$^+$Hep-2R cells. Treatment with either irradiation or GLUT-1 siRNA caused significant G0/G1 arrest and significantly reduced the proportions of cells in S and G2/M phases compared to controls. In comparison with the effects of irradiation alone, combined treatment with GLUT-1 siRNA and irradiation showed more significant effects on the cell cycle, as the proportion of cells in the G0/G1 phase was higher and those in the S and G2/M phases were lower. Therefore, we speculated that GLUT-1 siRNA enhanced the radiosensitivity of CD133$^+$Hep-2R cells through redistribution of the phases of the cell cycle. In Figure 2C, we demonstrated that there was significant difference in cell cycle phases among Hep-2, CD133$^+$-Hep-2, and CD133$^+$-Hep-2R and the reason for the above cell cycle distribution could be that CD133 promote the cell cycle progression of CD133$^+$-Hep-2 and CD133$^+$-Hep-2R.

Next, we analyzed the apoptosis rate of CD133$^+$-Hep-2R cells to determine whether GLUT-1 siRNA enhanced radiosensitivity by increasing irradiation-induced apoptosis. The combination of GLUT-1 siRNA and irradiation caused more apoptosis in CD133$^+$-Hep-2R cells than irradiation alone, both in vitro and in vivo. As DNA damage caused by irradiation is the major cause of apoptosis after radiotherapy, we postulated that GLUT-1 siRNA may have enhanced the radiosensitivity of CD133$^+$-Hep-2/2R cells by inhibiting DNA repair capability. Therefore, we examined the expression levels of RAD51 and DNA-PKcs in CD133$^+$-Hep-2R cells, both of which are known to participate in the major repair pathways involved in DSB repair. Combined treatment with GLUT-1 siRNA and irradiation reduced RAD51 and DNA-PKcs expression further than irradiation alone, both in vitro and in vivo. Accordingly, we speculated that GLUT-1 siRNA enhanced the radiosensitivity of CD133$^+$-Hep-2R cells by inhibiting DNA repair capability and increasing apoptosis.

It is widely accepted that the expression of GLUT-1 is regulated by the parthway of mammalian target of rapamycin (mTOR), for example, Gao et al found that in gastric cancer, mTOR/PKM2 and STAT3/c-Myc signaling pathways crosstalk to enhance the energy metabolism through up-regulating

the expression of GLUT-1;[37] Nakaigawa et al reported that in renal cell carcinoma, the expression of GLUT-1 was increased in the renal cell carcinoma cells surviving under hypoxia condition via mTOR pathway;[38] Sun et al reported that in Malignant perivascular epithelioid cell tumor, the up-regulation of mTOR leads to the up-regulation of GLUT-1;[39] Kavitha el al. Showed that in maternal nutrient restriction of baboon, the down-regulation of mTOR causes the down-regulation of GLUT-1.[40] From the above citation, it could be said that the mTOR pathway is the upstream regulator of the expression of GLUT-1, so it would be very interesting to further investigate the involvement of mTOR in the regulation of GLUT-1 in laryngeal cancer and this direction would be the important aim of our next research in the future.

Moreover, it has been reported that besides mTOR pathway (regulatory pathway for GLUT-1), glutamine is another important factor to regulate the growth of cancer cells and some special mechanisms of cancer cells to deal with glutamine deprivation can be exploited to treat some cancers, for example, Saqcena et al demonstrated that under glutamine deprivation, the breast cancer cell MDA-MB-231 (KRas driven cancer cells) could bypass the G1 late restriction point and enter S phase directly and then was arrested at S phase because of Insufficient nucleotide biosynthesis and at this time, these cancers are vulnerable to cytotoxic drugs such as capecitabine, paclitaxel, and rapamycin;[41–43] Gaglio et al reported that glutamine deprivation induces abortive s-phase rescued by deoxyribonucleotides in k-ras transformed fibroblasts;[44] Son et al reported that glutamine supports pancreatic cancer growth through a KRAS-regulated metabolic pathway.[45] Therefore, the pathway for glutamine metabolism and the pathway for glucose metabolism (mTOR, GLUT-1, etc.) are two independent factors to regulate certain cancers. This study currently only related to the glucose metabolism (GLUT-1) and it would be very interesting to investigate the potential crosstalk between GLUT-1 and the pathway for glutamine metabolism in laryngeal cancer and this direction would be another important aim of our next research in the future.

Conclusions

The results of the present study suggest that GLUT-1 siRNA enhanced the radiosensitivity of $CD133^+$-Hep-2R cells by redistributing the phases of the cell cycle, inhibiting DNA repair capability, and increasing apoptosis. Further investigations of the molecular mechanisms underlying the effects of GLUT-1 on the development of radioresistance in laryngeal CSCs are warranted for the establishment of precision targeted therapy.

Abbreviations

DSBs, DNA double-strand breaks; HR, homologous recombination; NHEJ, non-homologous end-joining; GLUT-1, glucose transporter-1; AS-ODN, antisense oligonucleotide; siRNA, small interfering RNA; CSCs, Cancer stem cells; $CD133^+$-Hep-2, Hep-2 laryngeal cancer cell line expressing high levels of CD133; Hep-2R, radioresistant Hep-2; $CD133^+$-Hep-2R, Hep-2R cells expressing high levels of CD133; CCK-8, Cell Counting Kit-8; MACS, magnetic-activated cell sorting; PBS, phosphate-buffered saline; RT-PCR, real-time polymerase chain reaction; PVDF, polyvinylidene difluoride; FITC, fluorescein isothiocyanate; PI, propidium iodide; ANOVA, analysis of variance; mTOR, mammalian target of rapamycin.

Ethics Approval And Informed Consent

This investigation was conducted in accordance with the ethical standards of the National Research Council's Guide for the Care and Use of Laboratory Animals. The study was approved by the institutional review board of The First Affiliated Hospital, College of Medicine, Zhejiang University (Hangzhou, Zhejiang, China).

Data Availability

Data sharing is not applicable to this article as no datasets were generated or analysed during the current study.

Acknowledgement

This research was supported by National Natural Science Foundation of China (No. 81372903), and Science and Technology Department of Zhejiang Province, China (No.2016C33144).

Author Contributions

Jiang-Tao Zhong completed the transfection of GLUT-1-siRNA and wrote the manuscript in English. Qi Yu completed the RT-PCR, Western blot, and the collection of literatures. Shui-Hong Zhou revised the article. Er Yu completed the CCK-8 test, colony formation assay, transwell assay and the statistical analysis. Yang-Yang Bao completed the establishment of laryngeal tumor xenografts, measurement of body weight and xenograft tumor volume. Zhong-Jie Lu completed the X-irradiation of cells and laryngeal tumor xenografts. Jun Fan completed the immunomagnetic sorting and flow cytometry. All authors contributed to data analysis, drafting or revising the article,

gave final approval of the version to be published, and agree to be accountable for all aspects of the work.

Disclosure

The authors declare that they have no competing interests in this work.

References

1. Steuer CE, El-Deiry M, Parks JR, et al. An update on larynx cancer. *Cancer J Clin*. 2017;67(1):31–50.
2. Zhao H, Zhuang Y, Li R, et al. Effects of different doses of X-ray irradiation on cell apoptosis, cell cycle, DNA damage repair and glycolysis in HeLa cells. *Oncol Lett*. 2019;17(1):42–54. doi:10.3892/ol.2018.9566
3. Toulany M. Targeting DNA double-strand break repair pathways to improve radiotherapy response. *Genes*. 2019;10(1). doi:10.3390/genes10010025
4. Noda M, Ma Y, Yoshikawa Y, et al. A single-molecule assessment of the protective effect of DMSO against DNA double-strand breaks induced by photo-and gamma-ray-irradiation, and freezing. *Sci Rep*. 2017;7(1):8557. doi:10.1038/s41598-017-08894-y
5. Mueck K, Rebholz S, Harati MD, Rodemann HP, Toulany M. Akt1 stimulates homologous recombination repair of DNA double-strand breaks in a RAD51-dependent manner. *Int J Mol Sci*. 2017;18(11):2473. doi:10.3390/ijms18112473
6. Tekade RK, Sun X. The Warburg effect and glucose-derived cancer theranostics. *Drug Discov Today*. 2017;22(11):1637–1653. doi:10.1016/j.drudis.2017.08.003
7. Zhong JT, Zhou SH. Warburg effect, hexokinase-II, and radioresistance of laryngeal carcinoma. *Oncotarget*. 2017;8(8):14133–14146. doi:10.18632/oncotarget.13044
8. Pitroda SP, Wakim BT, Sood RF, et al. STAT1-dependent expression of energy metabolic pathways links tumour growth and radioresistance to the Warburg effect. *BMC Med*. 2009;7:68. doi:10.1186/1741-7015-7-68
9. Harada H. Hypoxia-inducible factor 1-mediated characteristic features of cancer cells for tumor radioresistance. *J Radiat Res*. 2016;57 Suppl 1:i99–i105. doi:10.1093/jrr/rrw012
10. Zhang TB, Zhao Y, Tong ZX, Guan YF. Inhibition of glucose-transporter 1 (GLUT-1) expression reversed Warburg effect in gastric cancer cell MKN45. *Int J Clin Exp Med*. 2015;8(2):2423–2428.
11. Zhou S, Wang S, Wu Q, Fan J, Wang Q. Expression of glucose transporter-1 and −3 in the head and neck carcinoma–the correlation of the expression with the biological behaviors. *ORL J Otorhinolaryngol Relat Spec*. 2008;70(3):189–194. doi:10.1159/000124293
12. Li LF, Zhou SH, Zhao K, et al. Clinical significance of FDG single-photon emission computed tomography: computed tomography in the diagnosis of head and neck cancers and study of its mechanism. *Cancer Biother Radiopharm*. 2008;23(6):701–714. doi:10.1089/cbr.2008.0510
13. Luo XM, Xu B, Zhou ML, et al. Co-inhibition of GLUT-1 expression and the PI3K/Akt signaling pathway to enhance the radiosensitivity of laryngeal carcinoma xenografts in vivo. *PLoS One*. 2015;10(11):e0143306. doi:10.1371/journal.pone.0143306
14. Fang J, Zhou SH, Fan J, Yan SX. Roles of glucose transporter-1 and the phosphatidylinositol 3kinase/protein kinase B pathway in cancer radioresistance [review]. *Mol Med Rep*. 2015;11(3):1573–1581. doi:10.3892/mmr.2014.2888
15. Shen LF, Zhao X, Zhou SH, et al. In vivo evaluation of the effects of simultaneous inhibition of GLUT-1 and HIF-1alpha by antisense oligodeoxynucleotides on the radiosensitivity of laryngeal carcinoma using micro 18F-FDG PET/CT. *Oncotarget*. 2017;8(21):34709–34726. doi:10.18632/oncotarget.16671
16. Zhao F, Ming J, Zhou Y, Fan L. Inhibition of Glut1 by WZB117 sensitizes radioresistant breast cancer cells to irradiation. *Cancer Chemother Pharmacol*. 2016;77(5):963–972. doi:10.1007/s00280-016-3007-9
17. Bao YY, Zhou SH, Lu ZJ, Fan J, Huang YP. Inhibiting GLUT-1 expression and PI3K/Akt signaling using apigenin improves the radiosensitivity of laryngeal carcinoma in vivo. *Oncol Rep*. 2015;34(4):1805–1814. doi:10.3892/or.2015.4158
18. Yan SX, Luo XM, Zhou SH, et al. Effect of antisense oligodeoxynucleotides glucose transporter-1 on enhancement of radiosensitivity of laryngeal carcinoma. *Int J Med Sci*. 2013;10(10):1375–1386. doi:10.7150/ijms.6855
19. Bao YY, Zhou SH, Fan J, Wang QY. Anticancer mechanism of apigenin and the implications of GLUT-1 expression in head and neck cancers. *Future Oncol*. 2013;9(9):1353–1364. doi:10.2217/fon.13.84
20. Ayob AZ, Ramasamy TS. Cancer stem cells as key drivers of tumour progression. *J Biomed Sci*. 2018;25(1):20. doi:10.1186/s12929-018-0426-4
21. Roato I, Ferracini R. Cancer stem cells, bone and tumor microenvironment: key players in bone metastases. *Cancers*. 2018;10(2).
22. Corro C, Moch H. Biomarker discovery for renal cancer stem cells. *J Pathol Clin Res*. 2018;4(1):3–18. doi:10.1002/cjp2.v4.1
23. Dai XM, Yang SL, Zheng XM, Chen GG, Chen J, Zhang T. CD133 expression and alpha-fetoprotein levels define novel prognostic subtypes of HBV-associated hepatocellular carcinoma: a long-term follow-up analysis. *Oncol Lett*. 2018;15(3):2985–2991. doi:10.3892/ol.2017.7704
24. Wei X, He J, Wang J, Wang W. MPEG-CS/Bmi-1RNAi nanoparticles synthesis and its targeted inhibition effect on CD133(+) laryngeal stem cells. *J Nanosci Nanotechnol*. 2018;18(3):1577–1584. doi:10.1166/jnn.2018.14303
25. Wang J, Wu Y, Gao W, et al. Identification and characterization of CD133(+)CD44(+) cancer stem cells from human laryngeal squamous cell carcinoma cell lines. *J Cancer*. 2017;8(3):497–506. doi:10.7150/jca.17444
26. Chen XH, Bao YY, Zhou SH, Wang QY, Wei Y, Fan J. Glucose transporter-1 expression in CD133+ laryngeal carcinoma Hep-2 cells. *Mol Med Rep*. 2013;8(6):1695–1700. doi:10.3892/mmr.2013.1740
27. Tang T, Zhou FX, Lei H, et al. Increased expression of telomere-related proteins correlates with resistance to radiation in human laryngeal cancer cell lines. *Oncol Rep*. 2009;21(6):1505–1509. doi:10.3892/or_00000381
28. Wu F, Hu Y, Long J, et al. Cytotoxicity and radiosensitization effect of TRA-8 on radioresistant human larynx squamous carcinoma cells. *Oncol Rep*. 2009;21(2):461–465.
29. Prince ME, Sivanandan R, Kaczorowski A, et al. Identification of a subpopulation of cells with cancer stem cell properties in head and neck squamous cell carcinoma. *Proc Natl Acad Sci U S A*. 2007;104(3):973–978. doi:10.1073/pnas.0610117104
30. de Jong MC, Pramana J, van der Wal JE, et al. CD44 expression predicts local recurrence after radiotherapy in larynx cancer. *Clin Cancer Res*. 2010;16(21):5329–5338. doi:10.1158/1078-0432.CCR-10-0799
31. Shen L, Zhang R, Sun Y, Wang X, Deng AM, Bi L. Overexpression of HSBP1 is associated with resistance to radiotherapy in oral squamous epithelial carcinoma. *Med Oncol*. 2014;31(6):990. doi:10.1007/s12032-014-0990-8
32. Felthaus O, Ettl T, Gosau M, et al. Cancer stem cell-like cells from a single cell of oral squamous carcinoma cell lines. *Biochem Biophys Res Commun*. 2011;407(1):28–33. doi:10.1016/j.bbrc.2011.02.084
33. Reid PA, Wilson P, Li Y, Marcu LG, Bezak E. Current understanding of cancer stem cells: review of their radiobiology and role in head and neck cancers. *Head Neck*. 2017;39(9):1920–1932. doi:10.1002/hed.v39.9
34. Seshacharyulu P, Baine MJ, Souchek JJ, et al. Biological determinants of radioresistance and their remediation in pancreatic cancer. *Biochim Biophys Acta Rev Cancer*. 2017;1868(1):69–92. doi:10.1016/j.bbcan.2017.02.003
35. Nicolay NH, Lopez Perez R, Saffrich R, Huber PE. Radio-resistant mesenchymal stem cells: mechanisms of resistance and potential implications for the clinic. *Oncotarget*. 2015;6(23):19366–19380. doi:10.18632/oncotarget.4358

36. Schwartz JL, Rotmensch J, Giovanazzi S, Cohen MB, Weichselbaum RR. Faster repair of DNA double-strand breaks in radioresistant human tumor cells. *Int J Radiat Oncol Biol Phys*. 1988;15(4):907–912. doi:10.1016/0360-3016(88)90125-3
37. Gao S, Chen M, Wei W, et al. Crosstalk of mTOR/PKM2 and STAT3/c-Myc signaling pathways regulate the energy metabolism and acidic microenvironment of gastric cancer. *J Cell Biochem*. 2018. [Epub ahead of print]. doi:10.1002/jcb.26915
38. Nakaigawa N, Kondo K, Ueno D, et al. The acceleration of glucose accumulation in renal cell carcinoma assessed by FDG PET/CT demonstrated acquisition of resistance to tyrosine kinase inhibitor therapy. *BMC Cancer*. 2017;17(1):39. doi:10.1186/s12885-016-3044-0
39. Sun L, Sun X, Li Y, et al. The role of (18)F-FDG PET/CT imaging in patient with malignant PEComa treated with mTOR inhibitor. *Onco Targets Ther*. 2015;8:1967–1970. doi:10.2147/OTT.S85444
40. Kavitha JV, Rosario FJ, Nijland MJ, et al. Down-regulation of placental mTOR, insulin/IGF-I signaling, and nutrient transporters in response to maternal nutrient restriction in the baboon. *FASEB J*. 2014;28(3):1294–1305. doi:10.1096/fj.13-242271
41. Saqcena M, Patel D, Menon D, et al. Apoptotic effects of high-dose rapamycin occur in S-phase of the cell cycle. *Cell Cycle*. 2015;14(14):2285–2292. doi:10.1080/15384101.2015.1046653
42. Saqcena M, Mukhopadhyay S, Hosny C, et al. Blocking anaplerotic entry of glutamine into the TCA cycle sensitizes K-Ras mutant cancer cells to cytotoxic drugs. *Oncogene*. 2015;34(20):2672–2680.14. doi:10.1038/onc.2014.207
43. Mukhopadhyay S, Saqcena M, Foster DA. Synthetic lethality in KRas-driven cancer cells created by glutamine deprivation. *Oncoscience*. 2015;2(10):807–808. doi:10.18632/oncoscience.253
44. Gaglio D, Soldati C, Vanoni M, et al. Glutamine deprivation induces abortive s-phase rescued by deoxyribonucleotides in k-ras transformed fibroblasts. *PLoS One*. 2009;4(3):e4715. doi:10.1371/journal.pone.0004715
45. Son J, Lyssiotis CA, Ying H, et al. Glutamine supports pancreatic cancer growth through a KRAS-regulated metabolic pathway. *Nature*. 2013;496(7443):101–105. doi:10.1038/nature12040